Research Article

Hongguo Yan, Rong Dai*, Bin Chen, Shunshe Luo, Yongmei Kang, Xinping Zhou, and Jinlian Pang

Sedimentary processes and patterns in deposits corresponding to freshwater lake-facies of hyperpycnal flow – An experimental study based on flume depositional simulations

https://doi.org/10.1515/geo-2022-0705
received May 17, 2024; accepted September 09, 2024

Abstract: The article establishes a depositional model for lacustrine hyperpycnal flow by examining dynamics, transport factors, and laminae formation. The results show that several typical experimental phenomena such as fluid front mixing, double flow division, underwater leap, water skiing, and "new head" can be observed in the flume experiment. Based on the experimental observation of the flow process, three modes of transport of hyperpycnal flow in freshwater lake basins are summarized: bottom-bed loading, suspended loading, and uplift loading. Further, the change of fluid properties in hyperpycnal flow is summarized in three stages: a high-concentration stage, a low-concentration stage, and an uplifting stage. There are two main factors affecting the long-range transport of hyperpycnal flow: (1) the concentration difference between the head deposits and the ambient water body and (2) shear force of turbulence in the upper part of hyperpycnal flow. The simulation experiments of hyperpycnites laminae show that the laminae change from continuous to intermittent with the increase of the transportation distance. It is clear that the mode of transport of the hyperpycnal flow has a controlling effect on the degree of development of the laminae. Eventually, a depositional model of lake-facies hyperpycnal flow under experimental conditions was constructed.

Keywords: sedimentation simulation experiment, hyperpycnal flow, hyperpycnites, depositional processes, depositional patterns

1 Introduction

Hyperpycnal flow is a kind of sediment gravity flow whose density is higher than that of environmental water. Hyperpycnal flow originated in the estuary during the flood period and flows along the bottom of the sedimentary basin under the action of gravity and exists in a quasi-steady state [1,2].

Hyperpycnal flow is a type of sedimentary fluid capable of transporting a large amount of sediment over long distances. Initially, many scholars believed that only suspended load existed in hyperpycnal flow [3,4]. However, as research deepened, it was found that they typically consist of three parts: suspended load, bed load, and floating load [5]; Zavala [6] studied the evolution process, sedimentary characteristics, and identification marks of different stages of hyperpycnal flow in detail, and according to these three transport modes, they divided the hyperpycnites into three lithofacies types according to its transportation mode. As the hyperpycnal flow deposition model is increasingly recognized by more and more people, many scholars believe that compared with the marine hyperpycnal flow, which has a large density difference with the water, continental lake basins with intense tectonic activity, sufficient basin depth, and small bottom area, and developed small rivers are more prone to forming lacustrine hyperpycnal flow [3–5]. In recent years, scholars in Shahejie Formation of the Dongying Depression in the Bohai Bay Basin [7,8],

* **Corresponding author: Rong Dai**, School of Physics and Optoelectronic Engineering, Yangtze University, Jingzhou, 434023, Hubei, China, e-mail: dairongyz88@126.com
Hongguo Yan: School of Geosciences, Yangtze University, Wuhan, 430100, Hubei, China
Bin Chen: 7th Oil Production Plant of PetroChian Changqing Oilfield Company, Xian, 710200, Shaanxi, China
Shunshe Luo: Cooperative Innovation Center of Unconventional Oil and Gas (Yangtze University), Wuhan, 430100, Hubei, China
Yongmei Kang: The 11th Oil Production Plant of Changqing Oilfield Branch of PetroChina, Qingyang, 745000, Gansu, China
Xinping Zhou, **Jinlian Pang:** Exploration and Development Research Institute of Changqing Oilfield Branch Company Ltd., PetroChina, Xian, 710018, Shanxi, China

the south Ordos Basin, central China [4], and the Lower Cretaceous Xiguayuan Formation of the Luanping Basin in Northeast China and other places have found evidence of hyperpycnal flow deposition in freshwater lake basin [7] and Dput forward the sedimentary model of hyperpycnal flow in freshwater lake basin [7]. And then, Xian et al. [9] established a model of the analysis of channelized hyperpycnal systems using outcrop information. To accurately understand the genesis and structure of lacustrine hyperpycnites deposits, it is necessary to conduct in-depth research on its dynamic mechanisms to better grasp its dominant control factors and developmental patterns [10–12]. Lamb and Mohrig [13] used a flume model to simulate the flow process of hyperpycnal flow, which evolves through a recirculation zone, a zone of limited depth flow, and a submersion zone before normal river water flows into a basin and reaches sufficient depth to form hyperpycnal flow. Jeffrey et al.'s [14] experiments showed that hyperpycnal flow can still form even under extremely low sediment concentrations, indicating that it is not just a special geological process but more of a common geological phenomenon. Boland's [15] experiment showed that the injection method, bottom slope, and settling velocity are critical factors affecting the hyperpycnal and hypopycnal plumes form. Although the research on the formation conditions and basic forms of hyperpycnal flow is relatively common, most of the studies are mainly based on marine basins, and there are fewer flume simulation experiments on the dynamic processes of lacustrine hyperpycnal flow dominated by fine-grained sediments and the characteristics of lacustrine hyperpycnites.

Flume sedimentation simulation experiments are an effective means to study the dynamics of fine-grained sedimentary processes and the distribution patterns of clay and sand [16–18]. In this article, by conducting flume sedimentation simulation experiments of hyperpycnal flow, we can well analyze the dynamic mechanisms of lacustrine hyperpycnal flow. Observations of the flow morphology characteristics, concentration changes, and sediment distribution patterns of hyperpycnal flow are made using camera monitoring and a laser particle size analyzer, with experimental data recorded. The dynamic processes and sediment distribution characteristics of lacustrine hyperpycnal flow are discussed, and a fine-grained sedimentary model for hyperpycnal flow deposition is established. This study can provide new perspectives for the research of hyperpycnal flow.

2 Experimental equipment and scheme

2.1 Simulation equipment and observational methods

The experiment was completed in the Ring Flume Simulation Laboratory of the Key Laboratory of Reservoir Development at Petro China. The experimental flume is overall semi-circular (as shown in Figure 1), with a depth of 60 cm, a width of 40 cm, two straight sections each 10 m long, and two semi-circular sections with a radius of 1.2 m, for a total length of 27 m. The side walls and bottom of the flume are made of high-strength, flat, tempered glass with excellent light transmission properties; the flume's framework is connected with a stainless steel structure, and the bottom is 1 m above the ground. The flume has excellent sealing properties, with no

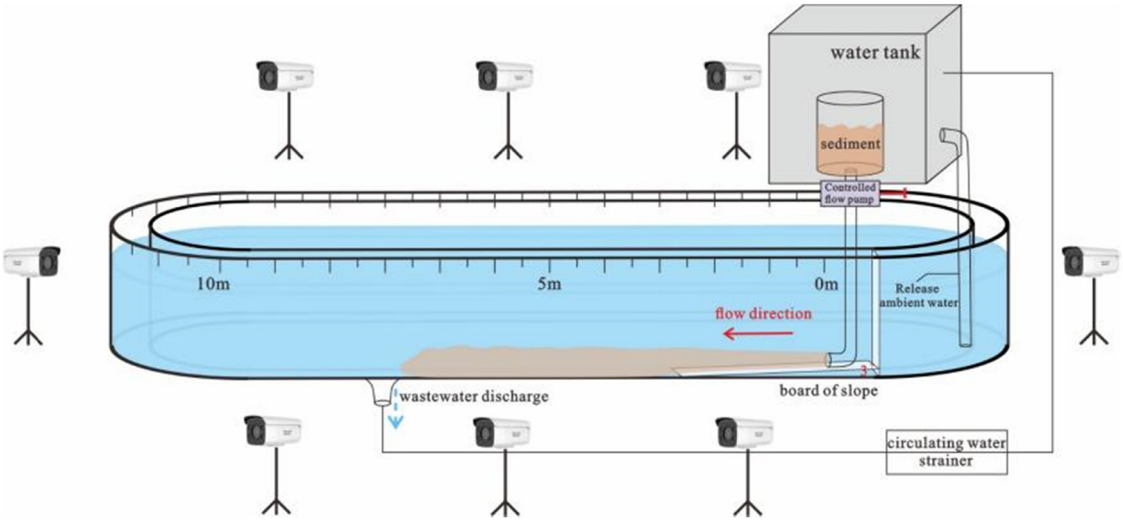

Figure 1: Schematic diagram of a circular flume and experimental equipment.

leakage, and is equipped with a 3 m^3 waste water pool in the middle of the ground to store and treat the water discharged during the experiment with sedimentation. The flume is also equipped with a 0.8 m^3 water storage tank for supplying water to the flume, which is 1.6 m above the ground, and the water storage tank has a water level control outlet and a water supply inlet. There is a cylindrical material storage bin equipped with a flow control valve, with a discharge rate controllable between 0.1 and 1 L/s. Using this system allows for the reproduction of the river impact process and achieves a level of controllability and adjustability, providing assistance in controlling experimental variables for subsequent experiments.

A slope adjustment plate is set up at the front 1.8 m of the flume. A high-definition, high-speed camera system is installed above the flume, which includes eight cameras to continuously capture images of the experimental process. This device enables real-time monitoring of the formation and deposition processes of hyperpycnal flow. The deposition process is an important measurement indicator in sediment simulation experiments. Real-time image monitoring of the experimental process allows for a comprehensive and intuitive record of the experiment. This can lead to the discovery of more experimental patterns through later comparison and interpretation of the experimental phenomena. A high-speed camera is also equipped to monitor the flow velocity of the fluid at different transportation distances in real time. The results after deposition are analyzed using a laser particle size analyzer to calculate the particle size distribution of the samples, with a testing range of 0.05–1,500 μm. By detecting parameters such as particle size and mass, the particle size distribution pattern of the sediments can be obtained.

2.2 Experimental plan

To simulate the depositional process of hyperpycnal flow within deepwater lake basins, the experiment was conducted in a static water environment. The design references the natural geographic environment of freshwater lake basins, including the bottom slope, the volume concentration range, and average flow velocity of natural hyperpycnal flow. It excludes the impact of climate and tectonic changes on sedimentation. The simulated river channel is designed to be 27 m long, 40 cm wide, with a slope set at 3°, a water depth of 0.35 m, a volume concentration of 5–20%, and an average flow velocity of 0.15 m/s (on a small scale). In the experiment, fine-grained sediments are selected, consisting of natural fine sand (<0.25 mm), silt (65–4 μm), and clay (<4 μm).

To explore the impact of fine-grained sediment mixture ratios on the flow velocity, transportation distance, and post-deposition outcomes of hyperpycnal flow, as well as the depositional process and patterns of lacustrine hyperpycnites, the experiment is divided into two groups: run 1: sand–clay ratio comparative experiment (Table 1) and run 2: hyperpycnites laminations simulation experiment (Table 2). The sand–clay ratio comparative experiment is a single-run experiment that compares the differences in the sediment flow process and post-deposition outcomes under different parameters for each experimental run, with a total of six runs designed. After each experiment, the flume is cleaned before proceeding to the next run; the laminar simulation experiment is a multi-run experiment, with a fixed slope of 3°, a water depth of 0.35 m, a total sediment volume of 50 L, a sediment concentration of 10%, and an initial flow velocity of 0.15 m/s. The

Table 2: Hyperpycnites laminations simulation experiment

Experimental run	Fine sand: silt: clay	Experimental run	Fine sand: silt: clay
Run 3–1	1:2:18	Run 3–8	1:2:12
Run 3–2	1:2:18	Run 3–9	1:2:6
Run 3–3	1:2:18	Run 3–10	1:2:6
Run 3–4	1:2:18	Run 3–11	1:2:6
Run 3–5	1:2:12	Run 3–12	1:2:6
Run 3–6	1:2:12	Run 3–13	1:2:6
Run 3–7	1:2:12	Run 3–14	1:2:6

Table 1: Sand–clay ratio comparative experiment

No.	Slope (°)	Water depth (m)	Total sediment amount (L)	Sediment concentration (%)	Initial flow velocity (m/s)	Sand–clay ratio (fine sand: silt: clay)
Run 1–1	3	0.35	25	5	0.15	1:2:6
Run 1–2						1:2:12
Run 1–3						1:2:18
Run 1–4	3	0.35	25	20	0.15	1:2:6
Run 1–5						1:2:12
Run 1–6						1:2:18

experiment uses a method of single release and multiple superimpositions, with a total of 14 runs designed.

2.3 Experimental method

During the simulation process, the sediment that has been evenly mixed is transported from the storage bin to the ring-shaped glass flume through a pipeline. After entering the flume, the sediment first passes through a 2 m slope zone and is then continuously transported forward. To facilitate the observation and recording of the fluid's motion state and the laws of change during the experimental process, a high-definition camera is used to record the experiment in real time. After the experiment, the thickness of the sediment is measured at every 1 m interval, and sediment samples are extracted using an underwater sampling method. A laser particle size analyzer is used to perform particle size analysis on the sediment samples, providing data support for the analysis of the distribution of hyperpycnal flow deposits. Based on the deposition thickness of the sediment at various stages and the results of the particle size analysis, a thorough study is conducted on the correspondence between the process and the results, followed by analysis. The experiment is divided into two phases, with a total of 20 runs completed.

3 Simulation of experimental process and observations of hyperpycnal flow

3.1 Single-phase experimental process

When the entire bin of sediment is suddenly released into the flume, the fluid as a whole exhibits a turbulent state, with a relatively uniform concentration and a height between 8 and 20 cm. At the initial stage of flow, the bottom layer flow of the hyperpycnal flow is initially entirely turbulent, and when the fluid flow becomes stable, it is composed of two parts: a rapidly moving laminar flow and a slowly moving turbulent flow, which transports sediment through rapid inertial flow [18]. During the transportation process, the fluid mixes with the ambient water, and when the head of the fluid gradually decreases in concentration to a critical point, a skimming flow action occurs [19–21]. The distance between the fluid head and the bed slowly increases, a skimming layer appears, and as the fluid is continuously diluted and thins by the surrounding water body, the head concentration gradually decreases. The fluid head changes from a tongue-like shape to a cloud-like shape, detaching from the bottom of the flume, lifting upward, and continuing to be rapidly transported forward [22–25].

When the fluid concentration gradually decreases to the critical point, the distance between the fluid head and the bed slowly increases, and a skimming layer emerges. As the fluid is continuously diluted and thins by the surrounding water body, the concentration of the fluid head gradually decreases and it lifts upward. The fluid head gradually separates from the main body, and a "new head" slowly forms at the front end of the main body. The new head also has the characteristic of lifting upward, overlaying on the thin layer, and moving forward slowly.

3.2 Typical experimental phenomena

3.2.1 Dual flow separation

When the transportation distance of the hyperpycnal flow is between 1 and 1.8 m, the fluid undergoes a change in flow state, transitioning from a vigorous turbulent state to a gradually stable high-concentration hyperpycnal flow. It is composed of two layers of fluid in the vertical direction (Figure 2), with the upper layer having a lower content of sediment particles, mainly supported by the turbulence of the fluid, while the lower layer has a higher content of particles in the sediment, where the internal turbulence of the fluid is suppressed, and the sediment is mainly supported by the matrix strength, dispersive pressure, and buoyancy [26–29]. At this point, due to the highest concentration at the head of the hyperpycnal flow, the fluid relies on the concentration difference between the head and the ambient water body to gain the driving force to keep moving forward, resulting in the characteristic of a thicker head and a thinner body of the fluid [19].

3.2.2 Mixing action of fluid front

During the experimental process, the complex mixing action between the fluid front and the ambient fluid can be observed. The mixing action is divided into two forms: (1) billows and (2) clefts and lobes [10] (Figure 3a and b). (1) Billows: located in the upper part of the heavier fluid front, it is a shear flow where the fluid moves upward in a rolling motion (Figure 4) and (2) clefts and lobes: below the fluid nose, influenced by the shear force of the bottom shape, a complex mobile pattern is formed.

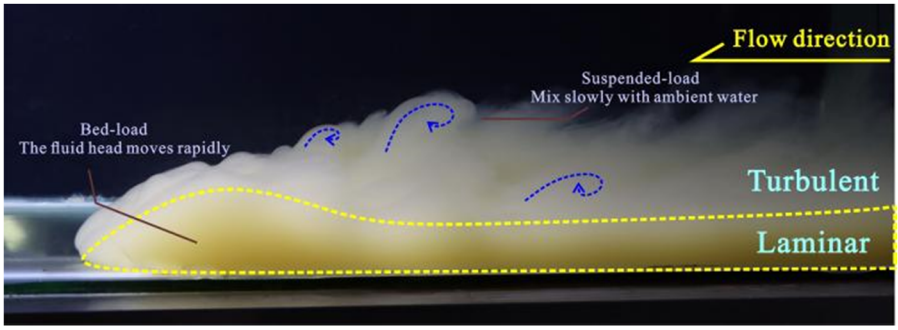

Figure 2: Dual flow bifurcation phenomenon in the hyperpycnal flow during the experimental process [24].

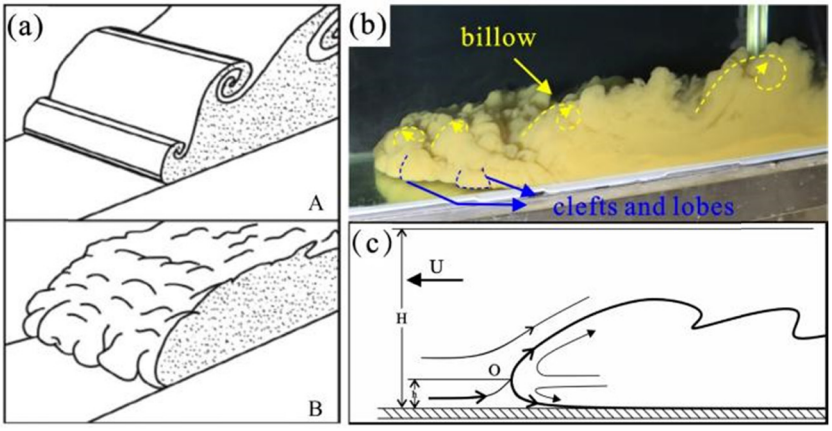

Figure 3: Fluid front mixing action. Notes: (a) mixing patterns of two gravity flow fronts [11]; (b) diagram of the mixing pattern experimental process; and (c) schematic diagram of the fluid front gravity flow state [10].

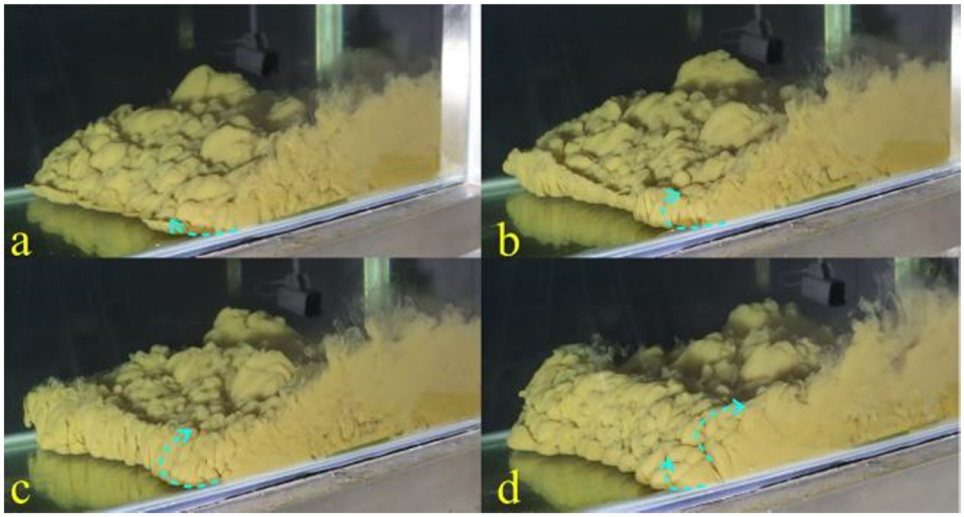

Figure 4: Wave action process during the experimental procedure. (a) The billow action just happened; (b) The billow rolls up; (c) The billow rolls backwards; and (d) The billow action happens consecutively.

Simpson [16] suggests that the mixing action beneath the fluid nose (clefts and lobes) is caused by gravitational instability due to the lighter fluid underlying the fluid nose. Under no-slip conditions, the bottom of the fluid front is affected by the frictional force with the ground, and its lowest streamlines extend towards the rear of the fluid, causing the stagnation point O to be lifted a certain distance. As a result, a small circulation of ambient fluid is created beneath the nose of the fluid front (in terms of height) (Figure 3c). The environmental fluid entering this area has a lower density than the fluid front above it, thus causing gravitational instability. As this part of the fluid rises and moves forward, it forms a structure of clefts and lobes.

Based on experimental observations, during the motion of the fluid, clefts absorb each other, and lobes rapidly expand or contract. When the lobes reach their maximum size, new clefts are formed. Experimental observations indicate that during a period of stable fluid flow, although the appearance and disappearance of clefts and lobes are very rapid, the total number of them generally remains constant over the corresponding transportation distance, representing the magnitude of the fluid's energy. There are more clefts and lobes in the proximal area of the hyperpycnal flow, and as the energy of the fluid flow decreases, the number of clefts and lobes correspondingly decreases until they disappear [16].

3.2.3 Underwater hydraulic jump

A hydraulic jump is the sudden transition of a fluid from supercritical to subcritical flow, characterized by a discontinuity or abrupt rise on the surface of the fluid. Its features include a sudden increase in fluid thickness, a sudden decrease in velocity, energy loss of the fluid, and a significant decrease in fluid density and sediment concentration [12–15]. Due to the significant reduction in fluid energy, intense sediment deposition occurs at the hydraulic jump and immediately downstream of it. The difference in fluid thickness before and after the occurrence of the hydraulic jump is referred to as the "jump height" [13] (Figure 5).

During the experimental process, the phenomenon of hydraulic jump frequently occurs in the near-source area. The essence of the hydraulic jump is the transformation of the form of fluid energy [17]. Before the jump, the energy is mainly kinetic, and after the jump, it is primarily potential. The hydraulic jump results in a significant loss of fluid energy. The hyperpycnal flow is strongly disturbed at the location of the hydraulic jump. In addition to the main flow continuing to move forward along the bottom, a series of rolls appear on the surface of the fluid, drawing a large amount of ambient water into the interior of the fluid, marking a strong phase of energy dissipation for the fluid.

3.2.4 Skimming flow effect leads to head elevation

Under experimental conditions, when the permeability of the debris flow is relatively poor, it can effectively resist the dilution of the fluid by the ambient water body. If the dynamic pressure of the debris flow exceeds the component of its own gravity along the slope downward, the head and the base contact area of the debris flow will invade a layer of liquid, causing the head of the debris flow to separate from the base. This reduces the shear drag on the head fluid and the base, allowing the debris flow to undergo rapid transportation. This phenomenon is known as the "skimming flow action" of the debris flow [14]. Previous studies have shown that although the skimming flow action is a possible explanation for the long-distance transportation of debris flows [23,24], experimental observations by David et al. [28] indicate that since the skimming flow action only occurs at the front of the debris flow and the range is only a few tens of centimeters, it can only act

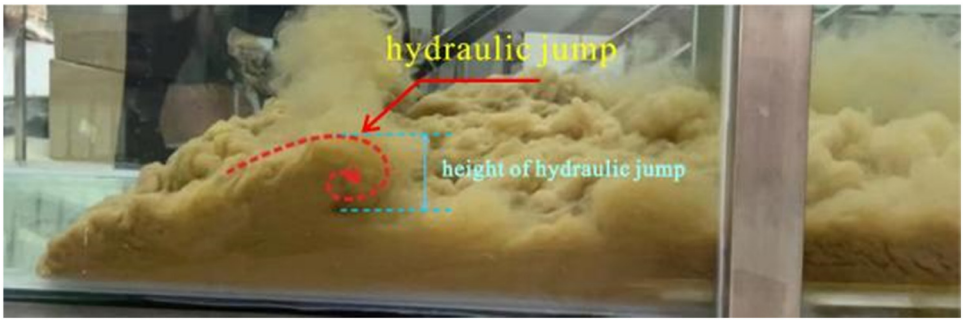

Figure 5: Underwater hydraulic jump phenomenon.

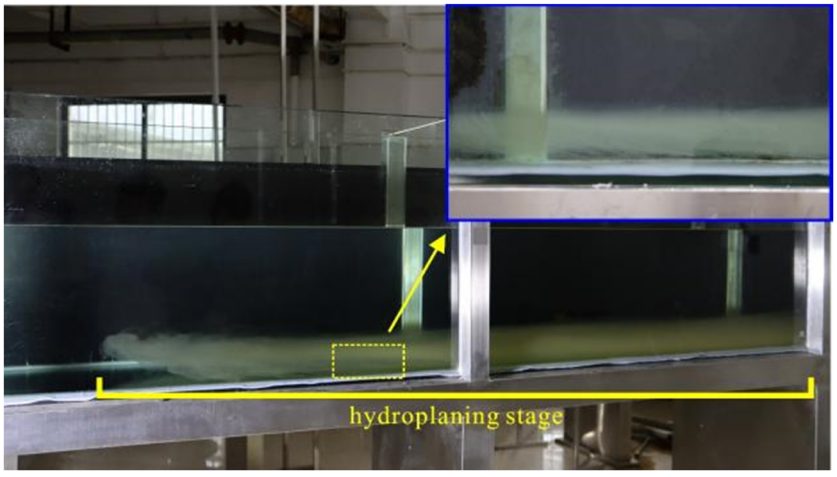

Figure 6: Skimming flow action phenomenon.

as a lubricating effect on the transportation of the head of the debris flow [24,25]. It does not ensure the long-distance transportation of the entire debris flow.

However, in this experiment of hyperpycnal flow, a long-distance skimming flow action was observed, with the skimming section being up to 1–1.5 m in length (Figure 6). Under the skimming flow action, as the fluid concentration gradually decreases to the critical point, the distance between the fluid head and the bed slowly increases, forming a layer of water film between the bottom of the fluid and the underlying water body, effectively reducing the bed frictional resistance. The fluid then accelerates over this layer of water film due to the force of gravity. As the fluid is continuously diluted and thinned by the surrounding water body, the concentration at the head of the fluid gradually decreases, changing from a tongue-like shape to a cloud-like shape, detaching from the bottom of the flume, lifting upward, and continuing to be rapidly transported forward (Figure 7).

3.2.5 New head uplifted phenomenon

During the sediment transport process, hyperpycnal flow is prone to skimming flow action. Under its influence, the fluid head is elevated, effectively reducing the frictional resistance of the bed. The fluid then accelerates over this layer of water film due to the force of gravity, resulting in the highest velocity at the fluid head. Consequently, the fluid head of the hyperpycnal flow tends to separate from the tail of the fluid, leading to the disintegration of the fluid. The separated head continues to be transported for a distance before depositing, a new fluid head continues to form, and the disintegration occurs continuously (Figure 8a–c). After deposition, scattered and isolated small sand bodies are formed around the lobes (Figure 8d).

In this experimental process, under the “skimming” action, the fluid head is elevated, and as the head lifts, it gradually separates from the main body. At this time, the head’s velocity will briefly accelerate, causing it to

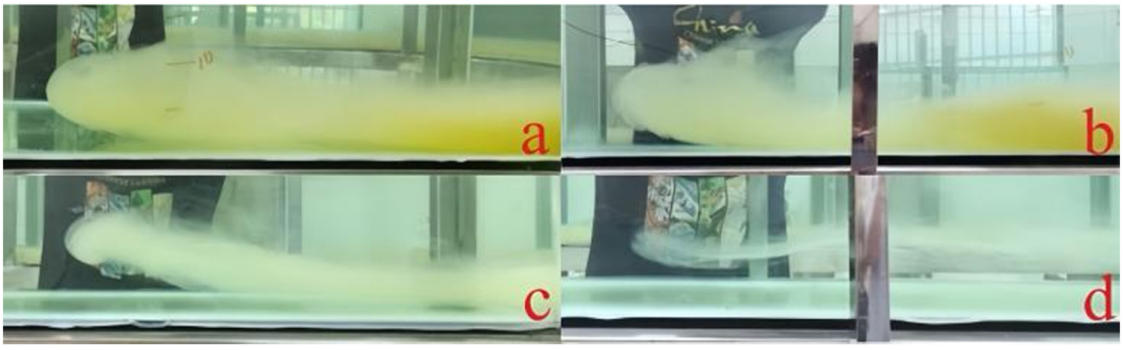

Figure 7: Head uplift diagram (a–d represent the morphological changes during the fluid head uplift process).

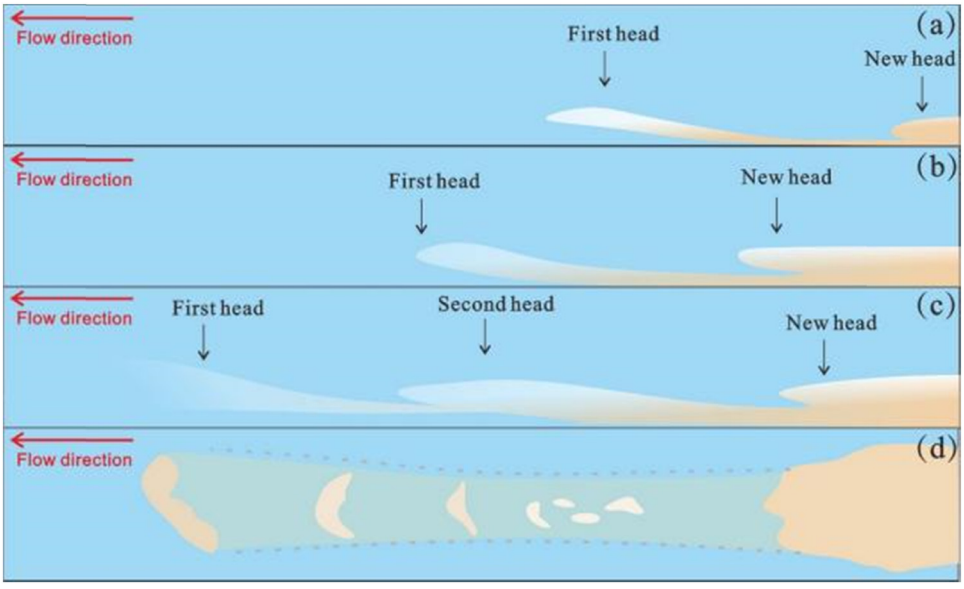

Figure 8: Schematic diagram of the "new head." Notes: (a)–(c) Schematic diagrams of the new head formation process and (d) schematic diagram of the "dispersive-type" sand body [30].

gradually pull away from the main body. A "new head" will slowly form at the front end of the main body. Compared to the first head, the new head has a smaller volume, a tongue-like shape, and a reduced concentration, but it shares the characteristic of upward lifting with the original head, overlaying on a thin layer and moving forward slowly (Figure 9). After the hyperpycnal flow undergoes "skimming," acceleration, and the head is lifted and moves for a period, new fluid heads continue to form, ultimately resulting in the formation of a "dispersive type" sand body [30].

4 Experimental results and discussion

During the simulation process, to facilitate the observation and recording of the motion state and the laws of change of the hyperpycnal flow during the experimental process, a high-definition camera is used to record the experiment in real-time throughout the process. After the experiment, the thickness of the sediment is measured at every 1 m interval, and sediment samples are extracted using an underwater sampling method. A laser particle size analyzer is used to perform particle size analysis on the sediment samples, providing data support for the analysis of the distribution of hyperpycnites [31,32]. Based on the deposition thickness of the sediment at various stages and the results of the particle size analysis, a thorough study is conducted on the correspondence between the process and the results, followed by analysis. The experiment is divided into two phases, with a total of 23 runs completed, accumulating approximately 500 h.

The experiment is a continuous hyperpycnal flow simulation. The first phase of the experiment is a sand–clay ratio comparative simulation experiment, consisting

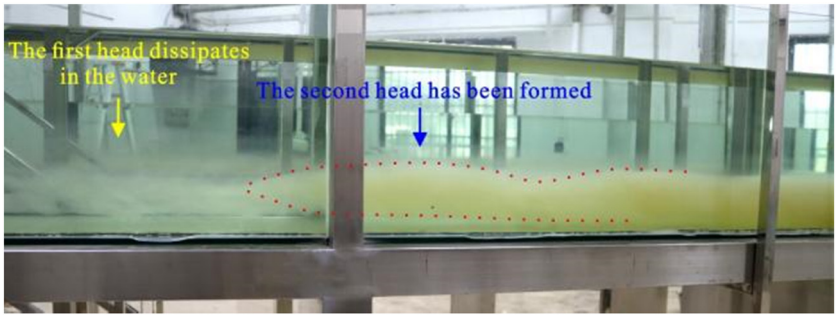

Figure 9: Two heads are connected through a thin layer.

of 6 runs, with a focus on observing the dynamic process of hyperpycnal flow during the experimental process and exploring the controlling effects of sediment concentration and sediment grain size variation on the distribution of sediments. The second phase of the experiment is a lamination simulation experiment, totaling 14 runs, where the stratification characteristics of the sediments after deposition are observed through multiple releases and superimpositions of the fluid, and the main controlling factors in the formation of hyperpycnal flow laminations are analyzed.

4.1 Transportation modes of lacustrine hyperpycnal flow

The transportation modes of hyperpycnal flow include three parts: suspended load, bed load, and floating load [28] (Figure 10). Based on the proportion of the three types of loads, hyperpycnal flow can be further categorized into those dominated by suspended load, those dominated by bed load, and those dominated by floating load. Generally, the floating part of the sediment in hyperpycnal flow is often found in the ocean, and there has been less attention paid to this by previous researchers. However, in this experiment, it was observed that the floating part of the sediment also exists in freshwater hyperpycnal flow.

4.2 Deposition dynamic process of hyperpycnal flow

Based on the transportation modes of hyperpycnal flow and combining the typical phenomena of this experiment, the changes in the fluid properties of hyperpycnal flow are divided into three stages: the high-concentration segment (strong dynamic stage) from 0 to 9 m; the low-concentration segment (stable flow stage) from 9 to 13 m; and the floating segment (head lifting – new head stage) from 13 m until the end of transportation.

(1) High-concentration segment (strong dynamic stage) from 0 to 9 m

In this stage, the hyperpycnal flow transportation mode is mainly dominated by the bed load component. As the transportation distance increases, coarse-grained sediments are gradually unloaded, resulting in a relatively large deposition thickness, with the sediment grain size gradually becoming finer from near to far.

When the fluid is released from the outlet, it is in a turbulent flow state without a specific form, and the concentration is relatively uniform at this time. In this stage, the relationship between the thickness of the sediment and the sand–clay ratio is the closest. At this point, a large amount of coarse particles such as clay pebbles in the sediment cannot be carried by the turbulence due to insufficient dynamics and are directly unloaded. Therefore, the sediment thickness is greatest in run 1–1 and run 1–4, which have the highest sand content (Figure 11).

After 2 m, the fluid gradually transitions from a high-speed turbulent state to a stable flow state. At this point, the fluid exhibits the same typical characteristics as the continuous high-density turbidity current – the coarse-grained sediments in the lower part are transported forward in the form of a laminar flow, while the fine-grained suspended sediments in the upper part of the fluid are characterized by being supported by turbulence.

During the 23 experimental runs, the underwater hydraulic jump phenomenon was highly developed, occurring in the 2–7 m section, and was more active closer to the

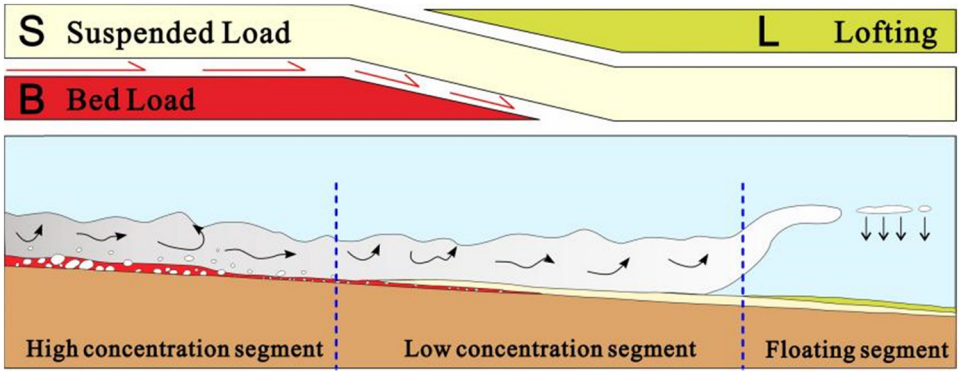

Figure 10: Transportation modes of lacustrine hyperpycnal flow (modified according to Reference [20]).

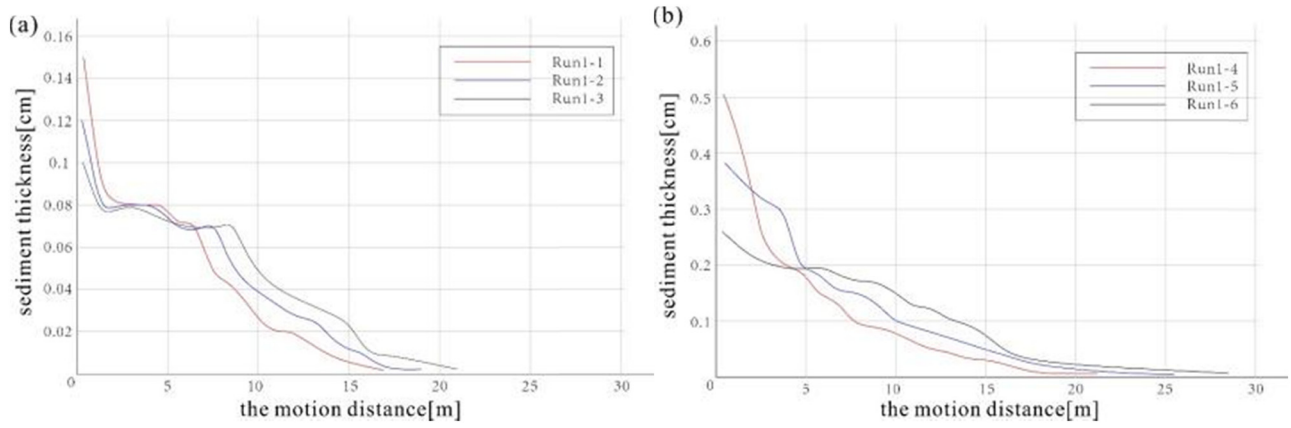

Figure 11: Comparison of sediment thickness in sand–clay ratio comparative experiments. Notes: (a) Line chart of sediment thickness in 5% concentration experiment and (b) line chart of sediment thickness in 20% concentration experiment.

sediment source area. It is characterized by discontinuity or an abrupt rise on the surface of the fluid, a sudden increase in fluid thickness, and a significant reduction in flow velocity. In the sand–clay ratio comparative experiments, the intensity of the hydraulic jump was greater in runs 1–4, 5, and 6 than in runs 1–1, 2, and 3. Since the essence of the hydraulic jump is the transformation of the form of fluid energy, it results in a substantial loss of fluid energy. Therefore, the rate of decrease in fluid velocity at this stage is relatively large (Figure 12), and the corresponding sediment deposition downstream of the hydraulic jump is more intense, leading to greater fluctuations in the thickness of the sediments deposited at this stage (Figure 11).

(2) Low-concentration segment (stable flow stage) from 9 to 13 m

The transition from the high-concentration segment to the low-concentration segment often occurs at the 9 m mark. After 9 m, as the transportation distance increases, the average velocity of the hyperpycnal flow shows a gradual decline due to the effect of the frictional force of the bed on the bottom boundary layer (Figure 12). At this stage, although the transportation speed of the hyperpycnal flow has slowed down, the overall shape remains clear and intact. As the coarse-grained material gradually deposits, the head's height decreases and the concentration is reduced [33,34]. Due to the weaker hydrodynamic force in this stage, the sediment particle size is relatively finer and is typically supported by turbulence, being transported in a suspended manner (Figure 13).

(3) The floating segment from 13 m until the end of transportation (head lifting – new head formation stage)

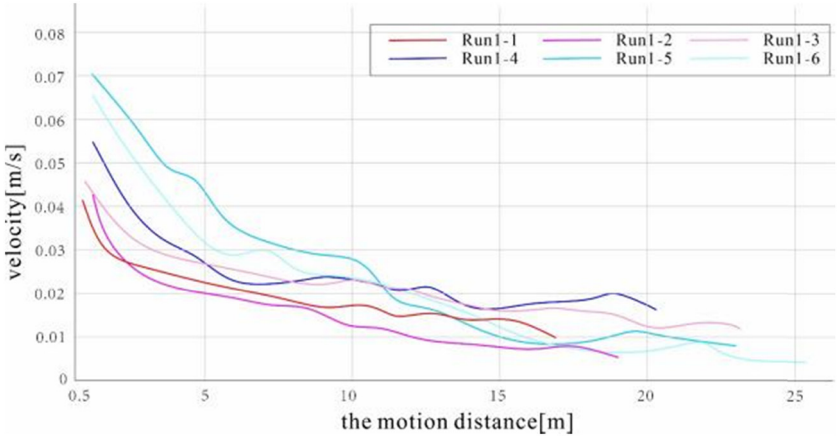

Figure 12: Line chart of fluid velocity in sand–clay ratio comparative experiment.

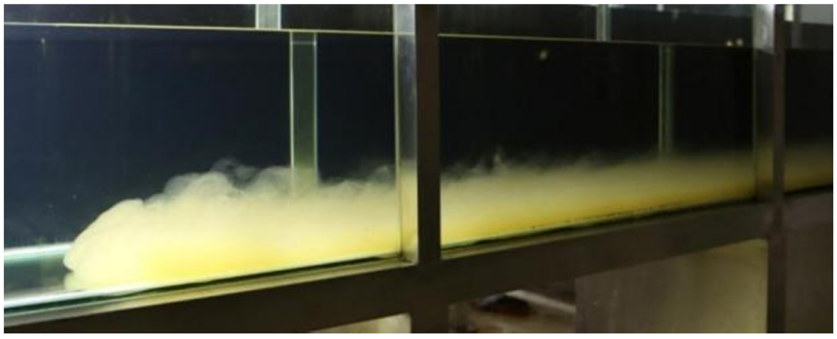

Figure 13: Phenomenon of hyperpycnal flow at 11 m.

At the 13 m mark, due to the continuous dilution by the environmental water, the concentration of the hyperpycnal flow continuously decreases until it reaches a critical point. At this point, the hyperpycnal flow often exhibits a phenomenon of head lifting under the action of skimming flow. After the head of the hyperpycnal flow is lifted, the viscous force between the head and the bed disappears, leading to a brief acceleration of the fluid velocity (Figure 11). Subsequently, as the head and the main body gradually separate and a "new head" continuously forms, the stage from the head lifting until the end of the single hyperpycnal flow is referred to as the floating segment.

4.3 Dominant control factors for the development of hyperpycnal flow

Based on the description of the aforementioned phenomena and the analysis of the experimental results, it is concluded that the main factors controlling the long-distance transportation of hyperpycnal flow are twofold: (1) the concentration difference between the head of the hyperpycnal flow and the ambient water body and (2) the shear force of the upper turbulence within the hyperpycnal flow.

(1) Concentration difference between the head of hyperpycnal flow and the ambient water body

Since the maximum concentration of hyperpycnal flow is mainly concentrated at the head, it relies primarily on the concentration difference with the surrounding water body to obtain the driving force for continuous advancement. When the sediment concentration is higher, the greater the concentration difference with the environmental water, the stronger the driving force obtained, and the farther the maximum distance of sediment transportation. During the experimental process, it can be observed by comparing the results of sand–clay ratio experiments with different concentrations: the greater the concentration of the hyperpycnal flow when released for the same amount of time, the farther the distance they are transported (Figure 12).

(2) Shear force of the upper turbulence in hyperpycnal flow

Comparison of transportation distances in sand–clay ratio comparative experiments among various groups: run 1–3 > run 1–2 > run 1–1; run 1–6 > run 1–5 > run 1–4 (Figure 14). From these data, it can be inferred that the higher the content of clay, the farther the hyperpycnal flow are transported.

The results of the sand–clay ratio comparative experiment show that: since the bed load component (coarse particles) of the hyperpycnal flow mainly relies on the shearing force of the turbulence at the upper part of the hyperpycnal flow for transportation, and both the low-concentration segment and the floating segment are transported in a turbulent state, the upper turbulent part is mainly composed of fine-grained sediments such as clay. Therefore, the higher the content of clay, the longer the turbulent characteristics can be maintained [30,31]. The clay material acts like a "skeleton" of the hyperpycnal flow, carrying coarser particles to a greater distance by wrapping and transporting them, thus allowing the sediments to be carried further away. Hence, the content of clay determines the magnitude of the shearing force of the upper turbulence of the hyperpycnal flow. The higher the clay content, the stronger the dragging effect of the turbulence, and the further the sediments are transported.

4.4 Hyperpycnites lamination distribution characteristics and dominant control factors

After the lamination experiment is concluded and the sediments have fully settled, the environmental water is

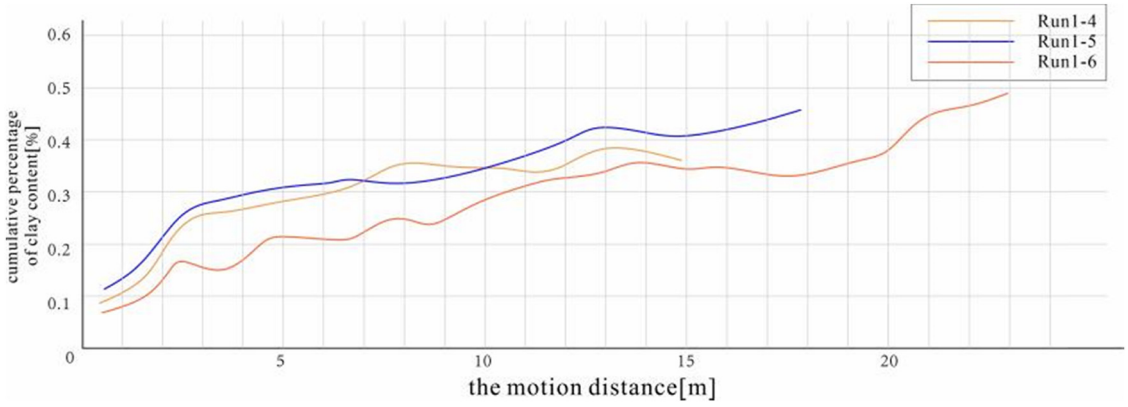

Figure 14: Percentage of clay content.

drained from above using the principle of siphoning (to prevent the sediment from floating, which would affect the experimental results). After the sediments have dried, samples are taken at fixed points every 1 m. The obtained slab samples are then analyzed using a stereomicroscope for side-section examination. To study their grain sequence and composition, the samples are impregnated with resin, ground into thin sections, and photographed using an optical microscope.

4.4.1 Sediment thickness distribution characteristics

Analysis of the thin-section results shows that the sediments near the water outlet (0–1.5 m) are quite mixed, with a coarser overall grain size, predominantly fine sand and coarse silt. After 1.5 m, the samples show uniform sediment deposition with the development of parallel lamination, presenting a clear interbedded sand–clay structure. Using a micrometer to measure the overall thickness of the sample and the thickness of the multiple small layers developed, the thickness variation pattern is ultimately determined: There are a total of 17 runs in the experiment, with measurement ranges between 0 and 19 m. According to the statistical results, the total thickness of the laminations decreases with increasing transportation distance (Figure 15).

4.4.2 Hyperpycnal flow's transportation methods' control on the development degree of lamination

As hyperpycnal flow moves from the near source to the far source, there is a loss of energy and a decrease in flow velocity, with the bed load, suspended load, and floating load being successively discharged, depositing in sequence to form a unique sedimentary sequence in the high-concentration segment, low-concentration segment, and floating segment. By comparing the thickness of laminations, sand–clay ratio (Figure 16), the thickness and number of sublayers, and combining with the thin-section photomicrographs of the lamination samples, the controlling effect of

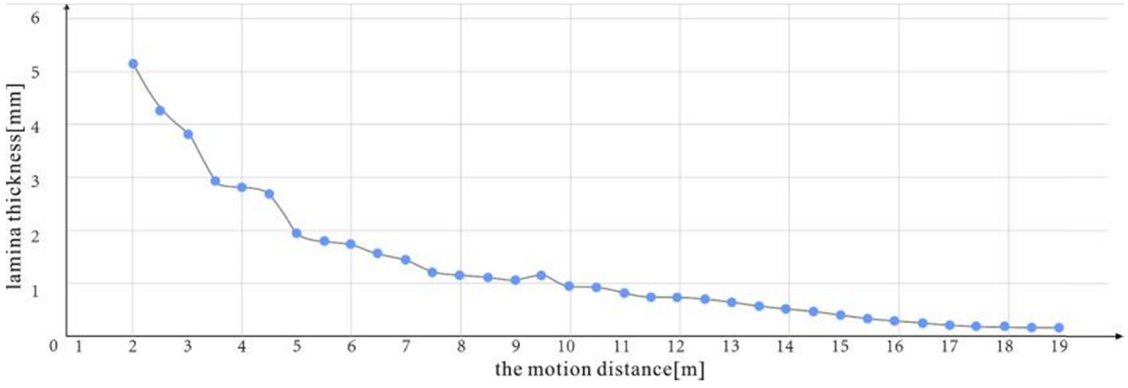

Figure 15: Statistical results of total thickness of hyperpycnites laminates.

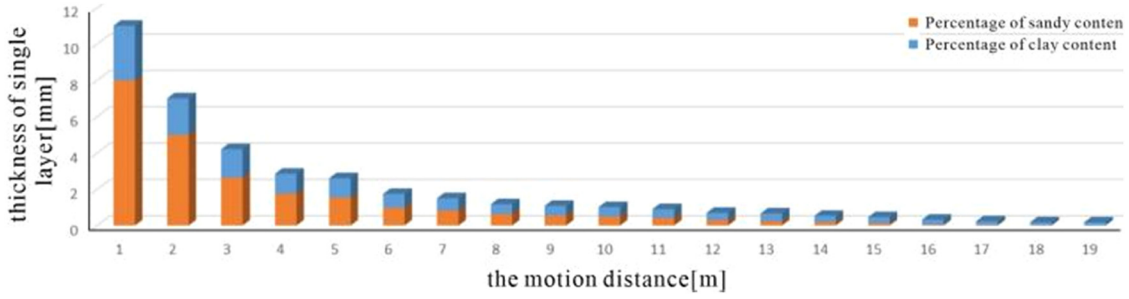

Figure 16: Comparison of clay and sand content in sediments.

the transportation modes of hyperpycnal flow on the development of laminations in the three stages of high-concentration, low-concentration, and floating segments is summarized (Figure 17).

(1) High-concentration segment (0–9 m)

In the 0–9 m segment, the average sand–clay ratio is 2:1. At this point, the sediment concentration is high, and the transportation mode is mainly bed load, which is the main unloading stage for coarse-grained sediments. At this time, the sand grain laminations and clay laminations are clearly interbedded (Figures 16 and 18a).

At the 9 m mark, the sand–clay ratio is 1:1, which is the critical point where the hyperpycnal flow transition from being dominated by bed load to being dominated by suspended load, with the content of sand and clay being essentially equal (Figures 16 and 18b).

(2) Low-concentration segment (9–13 m)

In the 9–13 m segment, the average sand–clay ratio is 1:2. At this point, the sediment concentration is low, and the transportation mode is mainly suspended load. There are fewer laminations, with some discontinuous laminations present, and a large amount of clay mixed with a small amount of silt is deposited (Figures 16 and 18c).

(3) Floating segment (13 m to the end of transportation)

From 13 m to the end of transportation, the average sand–clay ratio is 1:8. At this point, the sediment concentration is extremely low, and the main transportation mode is floating load. There are very few and discontinuous laminations, and the deposit is essentially pure clay (Figures 16 and 18d).

4.4.3 Distribution characteristics of hyperpycnites laminations

Near the discharge end, the sediments are quite mixed, with a coarser overall grain size, predominantly fine sand and coarse silt, including some clay materials. The cross-section shows continuous, superimposed lens-shaped channels (Figure 19a). When the sediments are transported to a distance of 2.5 m, they have not been excessively sorted, with a wide range of grain sizes and a dominance of coarse sediments. The laminar morphology of the hyperpycnal flow is continuous and the bedding is clear. Since the duration of a single release of hyperpycnal flow in the experiment is 6–8 min, the flood peak lasts long enough and the hydrodynamic force is strong enough to erode all the deposits before the flood peak, leaving only normally graded sedimentary units (Figure 19b). Starting from 5 m, a typical vertical sequence of hyperpycnal flow can be observed: upward-coarsening reverse grading units and upward-fining normal grading units appear in pairs, representing the strengthening and weakening stages of hyperpycnal flow, with the greatest grain size at the

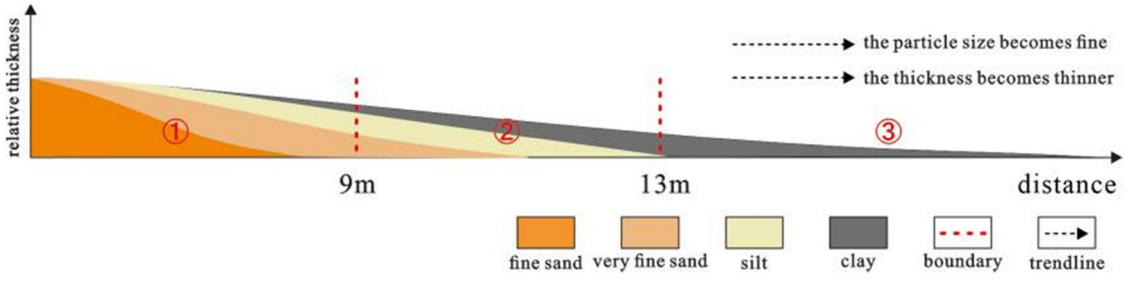

Figure 17: Schematic diagram of sediment distribution.

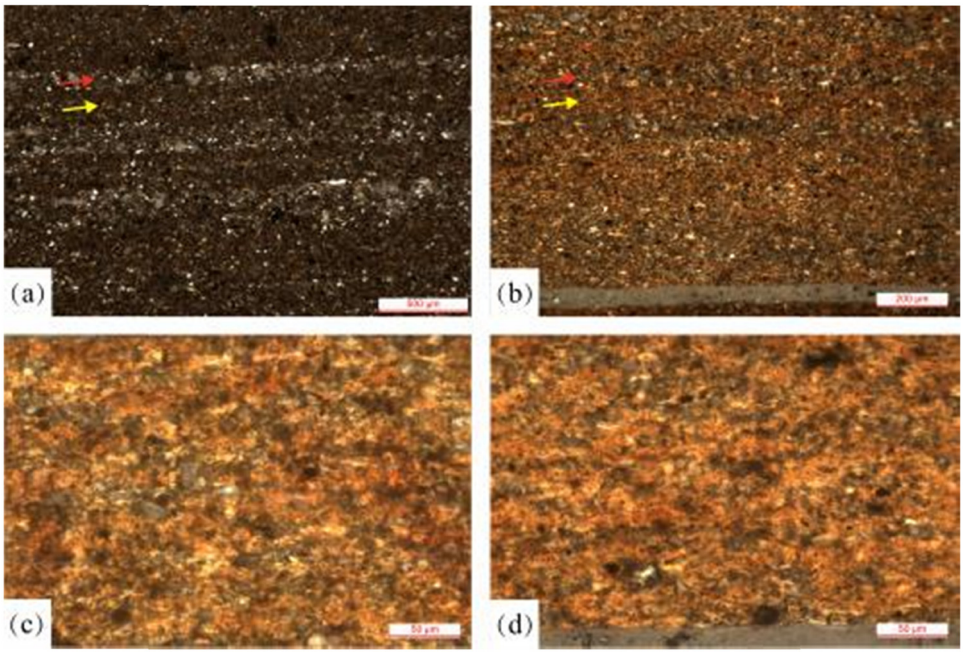

Figure 18: Hyperpycnites laminar thin section. (The red arrow is the sand layer; the yellow arrow is the clay layer.) Notes: (a) Laminations at 3 m, thin section (+); (b) laminations at 9 m, thin section (+); (c) laminations at 12 m, thin section (+); and (d) laminations at 17 m, thin section (+).

interlayer erosional contact surfaces (Figure 19c). At the farthest distance from the sediment source, the sediments are mainly clay with less sand content and weaker hydrodynamic force. At this point, the sediments are predominantly clay with rare discontinuous parallel lamination (Figure 19d). Therefore, the hyperpycnites laminations transition from a continuous to a discontinuous state with increasing transportation distance.

4.5 Deposition patterns of hyperpycnal flow

Fluids with a concentration greater than that of the basin water, capable of carrying a large and mixed load of sediment particles, which directly submerge into the low-concentration water body in the form of a flood and transport along the basin bottom over long distances, are known as hyperpycnal flow. Generally, the formation process

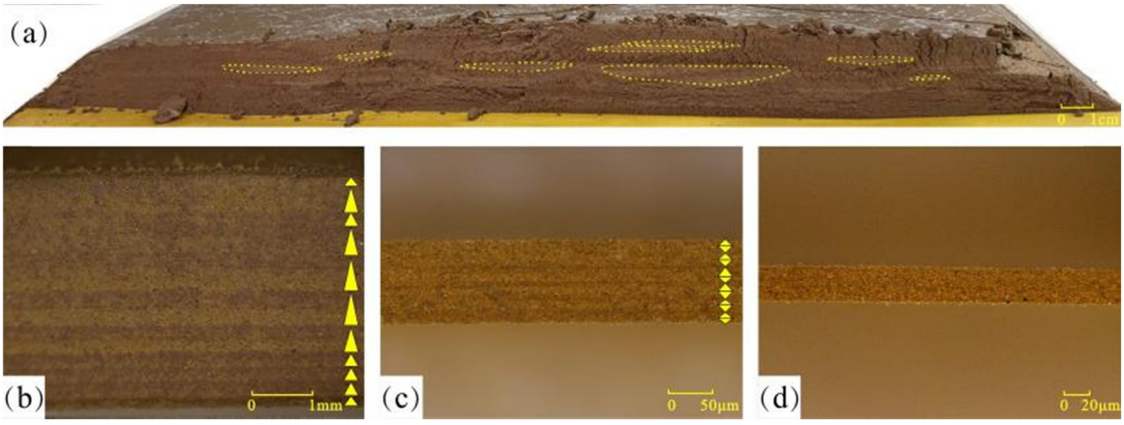

Figure 19: Vertical sequence of sediments at different transportation distances. Notes: (a) Longitudinal section of sediments at 1 m; (b) laminations at 3 m; (c) laminations at 9 m; and (d) laminations at 16 m.

(supply–transportation–deposition) of hyperpycnal flow in a basin is extremely complex and is controlled by a variety of environmental factors. Different geological backgrounds and environmental conditions correspond to hyperpycnal flow deposits with different characteristics. Based on the results and understanding from this flume experiment, and integrating the research findings of predecessors, the flow and depositional patterns of hyperpycnal flow under ideal conditions have been established (Figure 20).

The migration and evolution of hyperpycnal flow result in significant differences in sediment grain size among different depositional areas. The area near the water outlet, which is close to the sediment source, has strong hydrodynamic forces, dominated by erosional and filling deposition, resulting in coarser sediment grain sizes. In contrast, the far end has weaker hydrodynamic forces, predominantly clay sediments, and the middle area represents a transitional deposition of relatively coarse and fine sediments.

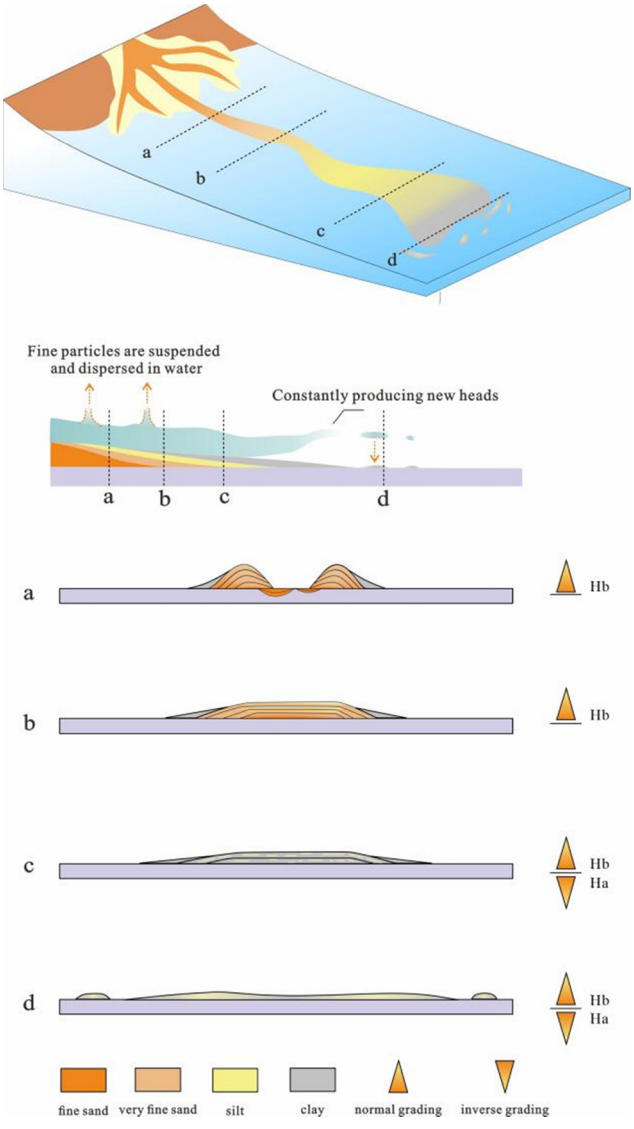

Figure 20: Deposition pattern diagram of lacustrine hyperpycnal flow. (a) Proximal end of the sediment source; (b) Middle to frontal proximal area of the sediment source; (c) Middle to rear proximal area of the sediment source; and (d) Distal end of the sediment source.

(a) Proximal end of the sediment source

At the proximal end of the sediment source, a high-concentration flood carries a large amount of sediment into the lake water. At this point, the hyperpycnal flow has just formed and possesses significant energy, being in the high-concentration segment of the hyperpycnal flow fluid. The sediment is predominantly coarse, mainly consisting of fine sand and clay pebbles, with a strong erosive effect on the underlying sediments, forming erosion channels. These channels can be filled with subsequent sediments, typically resulting in a normal grading sequence.

(b) Middle to frontal proximal area of the sediment source

In the middle to the frontal proximal area of the sediment source, which is the transitional zone from the continental slope to the basin center, the hyperpycnal flow deposits develop parallel lamination with clear and continuous forms. The topographic gradient changes from steep to gentle, and the depositional action of the hyperpycnal flow is intense. There is a significant unloading of coarse sediments, mainly fine sand, followed by silt, with a small amount of clay. Due to a stable supply of materials and a longer duration, coupled with strong hydrodynamic forces, all the deposits from before the flood peak are completely eroded, leaving only normally graded sedimentary units.

(c) Middle to rear proximal area of the sediment source

In the middle to rear proximal area of the sediment source, the energy of the hyperpycnal flow diminishes compared to the proximal end. The sediments gradually become finer and thinner towards the center of the basin, with silt and clay materials being predominant. The sediments are characterized by the development of typical reverse-to-normal grading sequences and intralayer micro-erosional surfaces. At this point, the lateral distribution range of the hyperpycnal flow gradually widens, and parallel lamination is more common but discontinuous.

(d) Distal end of the sediment source

At the distal end of the sediment source, which is the gentle central basin area, the flow velocity of the hyperpycnal flow is slow, and skimming flow action occurs. The deposition is primarily dominated by the continuously formed “new head.” The erosive action is weak, and lobate

deposits are formed at the terminus, with discontinuous small sand bodies distributed outside the lobes. The sediment grain size is finer, mainly clay, with a small amount of silt. Parallel lamination is rare and discontinuous, and the reverse-to-normal grading sequence is less pronounced than in the middle to rear proximal area.

5 Conclusion

(1) In the flume experiment process reproducing of hyperpycnal flow, many typical experimental phenomena can be observed. Combining the results of previous flume experiments, typical experimental phenomena such as bifurcation of dual flows, mixing action of the fluid front, underwater hydraulic jump, head lifting, and the "new head" uplifted phenomenon have been summarized. In-depth discussions have been conducted on the mechanisms of these phenomena.

(2) Through observation of the process of hyperpycnal flow, three transportation modes of hyperpycnal flow in freshwater basins have been summarized: bed load, suspended load, and floating load. Based on the transportation modes of hyperpycnal flow and combined with the typical phenomena of this experiment, the changes in the fluid properties of hyperpycnal flow are divided into three stages: the strong dynamic high-concentrated segment from 0 to 9 m; stable flow low-concentrated segment from 9 to 13 m; and the floating segment (head lifting – new head uplifted stage) from 13 m until the end of the transportation.

(3) Sand–clay ratio comparative experiments indicate that the main factors controlling the long-distance transportation of hyperpycnal flow are twofold: (1) The concentration difference between the head of the hyperpycnal flow and the ambient water body exerts a controlling effect on the transportation distance of the hyperpycnal flow; when the release time of the hyperpycnal flow is the same, the greater the concentration, the farther the transportation distance. (2) The shearing force of the turbulence at the upper part of the hyperpycnal flow also controls the transportation distance; the more clay content there is in the hyperpycnal flow, the farther they are transported.

(4) Results from the hyperpycnal flow laminar simulation experiments indicate that, in terms of laminar morphology, as the transportation distance increases, the hyperpycnites laminae transition from a continuous to a discontinuous state. During the process from the near-source to the far-source, there is a loss of energy and a decrease in flow velocity. The bed load, suspended load, and floating load are successively unloaded, and the high-concentration segment, low-concentration segment, and floating segment successively deposit to form a unique sedimentary sequence. Therefore, it is shown that the transportation mode of hyperpycnal flow has a controlling effect on the degree of laminar development.

(5) Based on the results of sand–clay ratio comparative experiments and the results of hyperpycnal flow laminar simulation experiments, combined with previous research on the depositional process of hyperpycnal flow, a unique depositional model for lacustrine hyperpycnal flow in the flume experiment mode has been established. The hyperpycnal flow exhibits a trend of gradually finer grain size and decreasing thickness from the near end to the mid-front end, mid-rear end, to the far end, and is capable of long-distance transportation.

Funding information: Research on the Technology of Increasing Reserves, Production, and Exploration and Development of Continental Shale Oil on a Large Scale, Group Company Tackling Applied Science and Technology Special Project, 2023ZZ15.

Author contributions: The author Hongguo Yan is responsible for the methodology of the article and drafted the initial manuscript. Rong Dai is responsible for the methodology and modified the content of the article. Bin Chen, Shunshe Luo, Yongmei Kang, Xinping Zhou, and Jinlian Pang participated in part of the experimental work and analysis of the results.

Conflict of interest: The authors declare that there is no conflict of interest regarding the publication of this article.

References

[1] Skene K, Mulder T, Syvitski J. Turbidity currents generated at river mouths during exceptional discharges to the world oceans. J Geol. 1995;103:285–99. doi: 10.1086/629747.

[2] Mulder T, Migeon S, Savoye B, Jouaneau J. Twentieth century floods recorded in the deep mediterranean sediments. Geology. 2001;29(11):1011–4. doi: 10.1130/0091-7613(2001)0292.0.CO;2.

[3] Zavala C, Ponce J, Arcuri M, Drittanti D, Freije H, Asensio M. Ancient lacustrine hyperpycnites: a depositional model from a case study in the rayoso formation (cretaceous) of West-Central Argentina. J Sediment Res. 2006;76(1):41–59. doi: 10.2110/jsr.2006.12.

[4] Plink-Bjoerklund P, Steel R. Initiation of turbidity currents: outcrop evidence for Eocene hyperpycnal flow turbidites. Sediment Geol. 2004;165(1–2):29–52. doi: 10.1016/j.sedgeo.2003.10.013.

[5] Mulder T, Chapron E. Flood deposits in continental and marine environments: character and significance. Vol. 61, 2011. p. 1–30. doi: 10.1306/13271348St613436.

[6] Zavala C. Hyperpycnal (over concentration) flows and deposits. J Palaeogeogr Engl. 2020;9(3):21. doi: 10.1186/s42501-020-00065-x.
[7] Wu Q, Xian B, Gao X, Tian R, Zhang H, Liu J, et al. Diversity of depositional architecture and sandbody distribution of sublacustrine fans during forced regression: A case study of Paleogene Middle Sha 3 member in dongying sag, bohai bay basin, East China. Pet Exploration Dev. 2023;50(4):894–908. doi: 10.1016/S1876-3804(23)60436-7.
[8] Yang K, Zhou D, Yang B, Tong J, Luo S, Chen Y, et al. The depositional evolution and controlling factors of the lower triassic baikouquan formation, Northern Mahu Slope, junggar basin, NW China. Geol J. 2021;56(5):2720–35. doi: 10.1002/gj.4064.
[9] Xian B, Wang J, Gong C, Yin Y, Chao CZ, Liu JP, et al. Classification and sedimentary characteristics of lacustrine hyperpycnal channels: Triassic outcrops in the south ordos basin, central China. Sediment Geol. 2018;52:S0037073818300460. doi: 10.1016/j.sedgeo.2018.03.006.
[10] Yang T, Cao Y, Liu H. Highstand sublacustrine fans: The role of a sudden increase in sediment supply. Basin Res. 2023;35(4):1486–1508. doi: 10.1111/bre.12762.
[11] Liu J, Xian B, Tan X, Zhang L, Su M, Wu Q, et al. Depositional process and dispersal pattern of a faulted margin hyperpycnal system: The eocene dongying depression, bohai bay basin, China. Mar Pet Geol. 2022;135:105405.
[12] Dou L, Hou J, Song S, Yang Y. Sedimentary characteristics of hyperpycnites in a shallow lacustrine environment: A case study from the lower cretaceous xiguayuan formation, luanping basin, Northeast China. Geol J. 2020;55(5):3344–60. doi: 10.1002/gj.3599.
[13] Lamb M, Mohrig D. Do hyperpycnal-flow deposits record river-flood dynamics? Geology. 2009;37(12):1067–70. doi: 10.1130/G30286A.1.
[14] Jeffrey G, Peter A, Shanmugam G, Gary P. Experiments on subaqueous sandy gravity flows: The role of clay and water content in flow dynamics and depositional structures. Geol Soc Am Bull. 2001;113(11):1–10. doi: 10.1130/0016-7606(2001)113<1377:E OSSGF>2.0.CO;2
[15] Boland T. An experimental and numerical investigation of hyperpycnal flow. Newark: University of Delaware; 2011.
[16] Simpson J. Effects of the lower boundary on the head of a gravity current. J Fluid Mech. 1972;53(4):759–68. doi: 10.1017/S0022112072000461.
[17] Simpson J. Gravity currents: In the Environment and the Laboratory. 2nd edn. Cambridge: Cambridge University Press; 1997. p. 1–244. doi: 10.1016/0012-8252(90)90057-3.
[18] Chow V. Open-channel hydraulics. New York: McGraw-Hill; 1959. p. 393–438. doi: 10.1016/0016-0032(60)90908-x.
[19] Cartigny M, Ventra D, Postma G, Van D, Jan H, Venditti J. Morphodynamics and sedimentary structures of bedforms under supercritical-flow conditions: New insights from flume experiments. Sedimentology. 2014;61(3):34–9. doi: 10.1111/sed.12076.
[20] Elverhoi A, Breien H, Blasio F, Harbitz C, Pagliardi M. Submarine landslides and the importance of the initial sediment composition for run-out length and final deposit. Ocean Dyn. 2010;60(4):1027–46. doi: 10.1007/s10236-010-0317-z.
[21] Komar P. Hydraulic jumps in turbidity currents. Geol Soc Am Bull. 1971;82(6):1477–88. doi: 10.1130/ 0016-7606(1971) 82[1477:HJITC] 2.0.CO;2.
[22] Kamalrulzaman K, Shalaby M, Islam M. Reservoir quality of the late cretaceous volador formation of the latrobe group, gippsland basin, Australia: Implications from integrated analytical techniques. Energy Geosci. 2024;5(1):100228. doi: 10.1016/j.engeos.2023.100228.
[23] Yu Q, Jia Y, Liu P, Hu X, Hao S. Rate transient analysis methods for water-producing gas wells in tight reservoirs with mobile water. Energy Geosci. 2024;5(1):100251. doi: 10.1016/j.engeos.2023.100251.
[24] Mutti E, Mavilla N, Angella S, Fava L. An introduction to the analysis of ancient turbidite basins from an outcrop perspective. AAPG Continuing Education Course Notes Series. Vol. 39, 1999. p. 34–8. doi: 10.1306/CE39687.
[25] Mutti E, Tinterri R, Benevelli G, Biase D, Cavanna G. Deltaic, mixed and turbidite sedimentation of ancient foreland basins. Mar Pet Geol. 2003;20(6–8):733–55. doi: 10.1016/j.marpet geo.2003.09.001.
[26] Zavala C, Arcuri M, Meglio M, Zorzano A, Espinosa L. A genetic facies tract for the analysis of sustained hyperpycnal flow deposits. In: Slatt RM, Zavala C, editors. Sediment transfer from shelf to deep water-revisiting the delivery system. Tulsa: AAPG; 2011. p. 31–51. doi: 10.1190/ice2016-6356637.1.
[27] Zavala C, Arcuri M, Valiente LB. The importance of plant remains as diagnostic criteria for the recognition of ancient hyperpycnites. Rev De Paleobiologie. 2012;11(6):457–69. doi: 10.1161/01.CIR.25.6.991.
[28] David M, Ellis C, Parker G, Whipple K, Hondzo M. Hydroplaning of subaqueous debris flows. Geol Soc Am Bull. 1998;110(3):387–94. doi: 10.1130/0016-7606(1998)110<0387:HOSDF>2.3.CO;2.
[29] Talling P. Hybrid submarine flows comprising turbidity current and cohesive debris flow: deposits, theoretical and experimental analyses, and generalized models. Geosphere. 2013;9(3):460–88. doi: 10.1130/GES00793.1.
[30] Pandey V, Chotaliya B, Bist N, Yadav K, Sircar A. Geochemical analysis and quality assessment of geothermal water in Gujarat, India. Energy Geosci. 2023;4(1):59–73. doi: 10.1016/j.engeos.2022.08.001.
[31] Lowe D. Sediment gravity flows: II depositional models with special reference to the deposits of high-density turbidity currents. J Sediment Petrol. 1982;52(1):279–97. doi: 10.1306/212F7F31-2B24-11D7-8648000102C1865D.
[32] Postma G, Nemec W, Kleinspehn K. Large floating clasts in turbidites: a mechanism for their emplacement. Sediment Geol. 1988;58(1):47–61. doi: 10.1016/0037-0738(88)90005-x.
[33] Ilstad T, Elverh I, Issler D, Marr J. Subaqueous debris flow behaviour and its dependence on the sand/clay ratio: a laboratory study using particle tracking. Mar Geol. 2004;213(1–4):415–38. doi: 10.1016/j.margeo.2004.10.017.
[34] Zheng W, Yin G, Sun L, Wei S, Wei X, Niu B. Sedimentary systems of the oligocene huagang formation in the central anticline zone of the Xihu depression, East China sea shelf basin. Energy Geosci. 2024;5(1):100150. doi: 10.1016/j.engeos.2022.100150.